Damage tolerance reliability analysis combining Kriging regression and support vector machine classification

Rudy Chocat, Paul Beaucaire, Loïc Debeugny, Jean-Pierre Lefebvre, Caroline Sainvitu, Piotr Breitkopf, Eric Wyart

▶ To cite this version:

Rudy Chocat, Paul Beaucaire, Loïc Debeugny, Jean-Pierre Lefebvre, Caroline Sainvitu, et al.. Damage tolerance reliability analysis combining Kriging regression and support vector machine classification. Engineering Fracture Mechanics, 2019, 216, pp.106514. 10.1016/j.engfracmech.2019.106514 . hal-03328337

HAL Id: hal-03328337

https://hal.utc.fr/hal-03328337

Submitted on 25 Oct 2021

HAL is a multi-disciplinary open access archive for the deposit and dissemination of scientific research documents, whether they are published or not. The documents may come from teaching and research institutions in France or abroad, or from public or private research centers.

L'archive ouverte pluridisciplinaire HAL, est destinée au dépôt et à la diffusion de documents scientifiques de niveau recherche, publiés ou non, émanant des établissements d'enseignement et de recherche français ou étrangers, des laboratoires publics ou privés.

Distributed under a Creative Commons Attribution - NonCommercial 4.0 International License

Version of Record: https://www.sciencedirect.com/science/article/pii/S0013794418303680
Manuscript_594ca969aeaca9553d71b3422381042b

Damage tolerance reliability analysis combining Kriging regression and support vector machine classification

Rudy Chocat[a,b,d,*], Paul Beaucaire[b], Loïc Debeugny[a], Jean-Pierre Lefebvre[b], Caroline Sainvitu[c], Piotr Breitkopf[d], Eric Wyart[c]

[a] *ArianeGroup, Forêt de Vernon, 27204 Vernon, France*
[b] *Cenaero France, 462 rue Benjamin Delessert, 77554 Moissy-Cramayel, France*
[c] *Cenaero, Rue des Frères Wright 29, 6041 Charleroi, Belgique*
[d] *Laboratoire Roberval, FRE2012 UTC-CNRS, Université de Technologie de Compiègne, 60203 Compiègne, France*

Abstract

Damage tolerance analysis associates a Fracture Mechanical model with the Failure Assessment Diagram to define the state of a space engine component. The reliability analysis treats the variability of numerical models assessing the probability of failure within Linear Elastic Fracture Mechanics (LEFM) hypotheses. However, these models, while providing quantitative information in the safe domain, give only qualitative information for failed components. This work proposes an original methodology to combine Kriging regression and the Support Vector Machine classification along with transition criteria between both approaches. To accurately describe the limit state, we define a specific enrichment strategy. The efficiency of the proposed methodology is illustrated on reference test cases.

Keywords: Damage Tolerance, Fracture Mechanics, Reliability, Kriging, Support Vector Machine, Subset Simulation

Nomenclature

d	Number of input random variables
$f_{\mathbf{X}}$	Joint density function of random vector $\mathbf{X}$
G	Performance function in the physical space
H	Performance function in the standard space
$\tilde{H}_{\mathrm{SVM}}$	SVM separator function
$\tilde{H}_{k_{\mathrm{SS}}}$	Surrogate of the performance function

*Corresponding author
Email address: rudy.chocat.pro@gmail.com (Rudy Chocat)

© 2019 published by Elsevier. This manuscript is made available under the CC BY NC user license
https://creativecommons.org/licenses/by-nc/4.0/

$\mathbb{I}$	Indicator function
k_{SS}	Index of the subset step
K	Stress Intensity Factor
K_r	Toughness criterion
K_{IC}	Toughness value
L_r	Remaining ligament criterion
M_{FAD}	Failure Assessment Diagram margin
n_{DOE}	Size of the DOE
n_{SS}	Size of the subset population
N_{cycle}	Number of cycles
N_{target}	Targeted number of cycles
p_f	Probability of failure
p_{target}	Targeted intermediate probability
$p_{k_{\mathrm{SS}}}$	Intermediate probability
P_{mc}	Probability of misclassification
$q_{\mathrm{th}}^{(k_{\mathrm{SS}})}$	Intermediate threshold
$\mathbf{U}$	Random vector in the standard space
$\mathbf{u}$	Realization of $\mathbf{U}$
$\mathbf{u}_{\mathrm{DOE}}$	DOE population
$\mathbf{u}_{\mathrm{SS}}$	Subset population
X	Random variable
$\mathbf{X}$	Random vector
$\phi_{\mathbf{U}}$	Multivariate Gaussian density function
$\bar{\sigma}_{\mathrm{nom}}$	Non-physical stress value of the remaining ligament
$\bar{\sigma}_{\mathrm{flow}}$	Second reference stress value depending on the material
$\bar{\sigma}_{\mathrm{ref}}$	First reference stress value depending on the material
AK	Adaptive Kriging
ARCSS	Adaptive Regression and Classification based on Subset Simulation
DOE	Design Of Experiments
FAD	Failure Assessment Diagram
FAL	Failure Assessment Line
LEFM	Linear Elastic Fracture Mechanics
MCS	Monte Carlo Simulation
SS	Subset Simulation
SVM	Support Vector Machine
XFEM	eXtended Finite Element Method

1. Introduction

In the aerospace sector, designing a component under damage tolerance hypotheses involves considering the structure as inherently flawed. It means that in a conservative way, each defect is considered as a crack and it is verified that the structure can withstand the loads throughout its lifetime. In space engine components context, a primary value of interest is the Failure Assessment Diagram (FAD) margin defined by the R6-rule [1]. If the FAD margin is positive, the component is considered as safe. Otherwise, it fails. The FAD is used in the post-processing phase of the crack analysis, performed by quickly evaluated analytical models or forms [2], but also by numerical approaches such as the extended finite element method (XFEM) [3, 4, 5] developed for complex structures.

However, as shown experimentally by Virkler [6], the crack propagation is subjected to uncertainties about geometry, material properties, loads [7] or considered defects [8]. The approach to set the properties to *the worth case* [9], even if it ensures the strength of the component, may generate over-sizing. Uncertainties may also be considered through probabilistic approaches [10]. The structural reliability provides, by setting stochastic models as inputs, the probability of failure which is required to be particularly low in the space application context [11].

In the low probability of failure assessment ($< 10^{-6}$) scope, the zone of interest is localized in the extreme tail of the distribution. Using Monte Carlo Simulation (MCS), the chance is meager to generate failed experiments which drive the convergence of the probability estimator. Therefore, in the FAD context [12], MCS is limited due to a large number of evaluations required to get accurate results. To limit the number of simulations, advanced reliability methods such as Subset Simulation (SS) [13] restrict the sampling to a subsequence of MCS, fixing the associated intermediate probability thresholds, until satisfaction of stopping criteria. The probability to generate failed experiments using SS is higher than with MCS reducing the variance of the estimators.

The use of Multi Level Monte Carlo approaches [14, 15], based on local derivative informations, strongly accelerates the Monte Carlo estimation. However, their intrusive character is limiting in the space engine application. Non intrusive multi-fidelity techniques [16, 17], mainly developed for optimization, are promising but they require high and low fidelity models.

The lack of quantitative information in the failure domain, resulting from the Linear Elastic Fracture Mechanics (LEFM) hypotheses, limits the application of gradient-based optimization methods such as FORM [18, 19], and SORM [20]. More sophisticated mechanical approaches such as plastification are omitted due to the use of dedicated model not required in the space engine component scope of this study. However, the same finding could be observed for any application for which post-failure behavior is not included within the working hypotheses. To treat the issue of computational cost, advanced reliability methods based on surrogates, also named meta-models, are built according to a Design Of Experiments (DOE) to cover the design space such as Latin Hypercube Sampling

(LHS) [21], Centroïdal Voronoï tessellation or "Latinized" Centroïdal Voronoï tessellation [22]. Even if the polynomial Response Surface Method [23, 24, 25] is one of the most popular approaches, the interest for Kriging grows for structural reliability [26, 27] due to the enrichment possibilities based on the underlying Gaussian process, such as ERGA [28] and Adaptive Kriging (AK) [29]. To assess low probabilities, methods such as AK-SS [30] and AK-SSIS [31] are adopted. However, these methods require a quantitative assessment of the FAD margin in both safe and failure domains. When only qualitative information, allowing only to qualify component as safe or unsafe, is available, classification methods based on Support Vector Machine (SVM) are preferable [32, 33]. As for Kriging, several enrichment strategies have been proposed in the SVM context. The Adaptive SVM [34] is based on the evaluation of a learning function whereas Max-Min [35] and Generalized Max-Min [36] solve an optimization problem. For low probability assessment, the 2SMART [37] method based on a succession of SVM separators, is proposed. We can note that the ASVR - SS [38] method uses the SVM for regression to assess low probabilities.

The present work proposes a specific procedure to assess the failure for damage tolerance using the FAD for Fracture Mechanics [1]. To our best knowledge, the existing surrogate-based reliability methods choose between regression and classification approaches. As the information is quantitative for safe components and qualitative for failed ones, the present work proposes to conjointly exploit regression and classification combining advantages of both approaches dealing, respectively, with continuous and binary information. Therefore, the key contribution of this paper is the definition of transition criteria between regression and classification phases. To achieve low probability, the proposed method is based on the subset simulation principle moving step by step to identify the limit state between the safe and failure domain. Moreover, in this contribution, an original adaptive strategy is explored to limit the number of model evaluations for the classification phase. The proposed methodology is called Adaptive Regression and Classification based on Subset Simulation (ARC-Subset).

The paper is organized as follows. The first section presents the damage tolerance analysis and introduces the definition of the probability of failure. The second section details the proposed ARC-Subset methodology starting with the regression phase. The classification phase is detailed with a new enrichment strategy based on the probability of misclassification [39]. Then, the transition between both phases is defined. In the last section, the methodology is applied to two test cases, based on the damage tolerance tool NASGRO [2], and compared with reference methods.

2. Reliability analysis for damage tolerance

This section introduces the concepts of damage tolerance for Fracture Mechanics and the notion of probability of failure.

2.1. Damage tolerance

The damage tolerance approach aims at ensuring component safety during a given number of cycles. In engineering practice, Fracture Mechanics models are often limited to the LEFM hypotheses for computational efficiency. At each step of the crack propagation, the outputs are processed considering failure scenarios depending on verification of two fracture criteria:

- the Stress Intensity Factor K attains the toughness K_{IC} value:

$$K_r = \frac{K}{K_{IC}} \leq 1, \tag{1}$$

- the surface between the crack front and the closest free surface, called 'remaining ligament' (see Figure 1), completely plastifies:

$$L_r = \frac{\bar{\sigma}_{\text{nom}}}{\bar{\sigma}_{\text{flow}}} \leq \frac{\bar{\sigma}_{\text{ref}}}{\bar{\sigma}_{\text{flow}}}, \tag{2}$$

  where $\bar{\sigma}_{\text{nom}}$ is a non-physical stress value resulting from loads applied on the remaining ligament. $\bar{\sigma}_{\text{ref}}$ and $\bar{\sigma}_{\text{flow}}$ are reference stress values depending on the material.

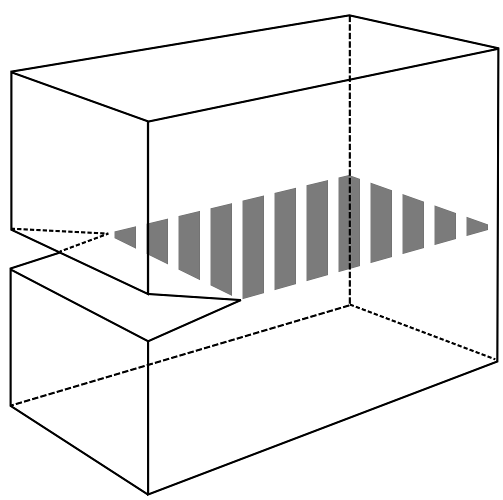

Figure 1: Illustration of the principle of the remaining ligament (dashed surface).

Both criteria (1) and (2) are correlated by the Failure Assessment Limit (FAL) which is the boundary between the 'accepted' and 'rejected' domains. In the Failure Assessment Diagram (FAD) shown in Figure 2, for K_r and L_r values reported as point A, the FAD margin M_{FAD} is defined as the distance ratio $|\text{OB}|/|\text{OA}|$ from the origin. In the cyclic loading, the targeted lifetime N_{target} is set. At each cycle i, $M_{\text{FAD}}(i)$ is evaluated. When point A crosses the FAL, the simulation is stopped, M_{FAD} is not available as the LEFM hypothesis

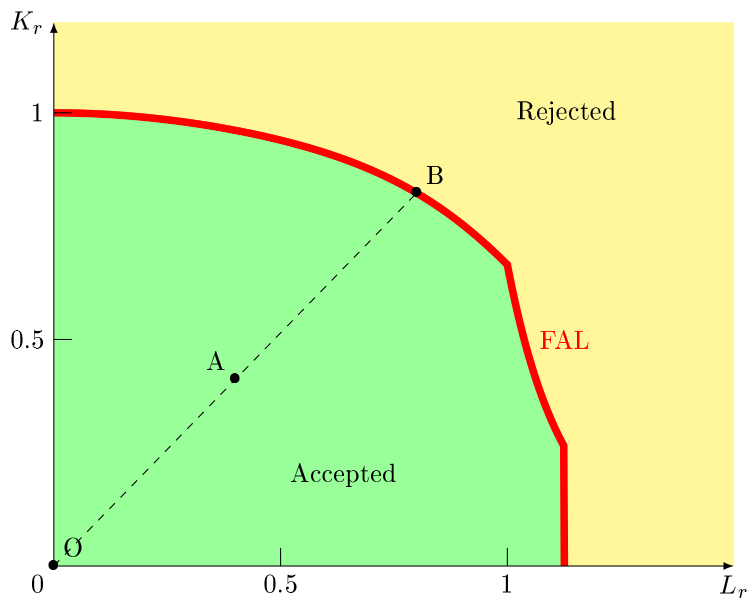

Figure 2: Failure Assessment Diagram (FAD) for damage tolerance in Fracture Mechanics. The red line is the Failure Assessment Limit (FAL). O is the origin of the FAD, point A is defined by (K_r,L_r) and B is the intersection between the FAL and (OA) allowing to compute M_{FAD}.

is not verified anymore, and the component is rejected. If the M_{FAD} remains positive at the end of the lifetime, the component is accepted. In Figure 3, the different steps of two crack propagation cases are illustrated: one for a safe component and one for a rejected one. Figure 4 illustrates the flowchart of the damage tolerance procedure. Therefore, a safe component is characterized by $N_{\text{cycle}} = N_{\text{target}}$ while a failed one by $N_{\text{cycle}} < N_{\text{target}}$. For the safe component, M_{FAD} is a positive quantity, while for the failed one, the obtained negative value is not representative beyond the LEFM hypothesis and may be considered only as qualitative.

2.2. Probability of failure

In the reliability context, the uncertainties are modeled by d random variables X which are defined using probability laws characterized by their distributions f_X. Random variables are combined in a random vector $\mathbf{X}$ of length d defined by a joint density function $f_{\mathbf{X}}$. A component is characterized by the performance function $G(\mathbf{X})$, $G(\mathbf{X}) > 0$ in the safe domain and $G(\mathbf{X}) \leq 0$ in the failure one. In the present work, the considered performance function is:

$$G(\mathbf{X}) = M_{\text{FAD}}(\mathbf{X}). \tag{3}$$

Different probability laws describe random, possibly correlated, variables at different scales in the physical space. The Nataf transformation moves $f_{\mathbf{X}}$ to $\phi_{\mathbf{U}}$

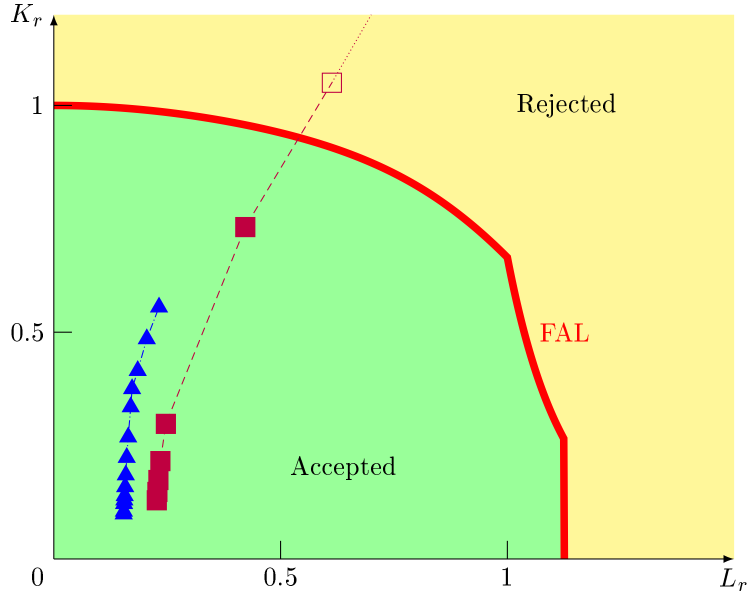

Figure 3: FAD: The dashed-dotted blue line with triangle markers shows the cycles for a safe component and allows the computation of the FAD margin at every step. The purple dashed line with square markers presents the steps of a failed component, the FAD margin is not quantifiable beyond the FAL with the LEFM hypothesis.

in the standard space where all input variables follow an uncorrelated normal distribution law with zero mean and unit standard deviation $\mathbf{U} \sim \mathcal{N}(0; \mathbf{I}_d)$. The performance function is mapped to the standard space $G(\mathbf{X}) \rightarrow H(\mathbf{U})$ divided into the *failure region* where $H(\mathbf{U}) < 0$, the *safe region* with $H(\mathbf{U}) > 0$ and the limit state $H(\mathbf{U}) = 0$.

The probability of failure is expressed as:

$$\begin{aligned} p_f &= P(G(\mathbf{X}) \leq 0) \\ &= \int_{G(\mathbf{X}) \leq 0} f_{\mathbf{X}} \mathrm{d}\mathbf{x} = \int_{H(\mathbf{U}) \leq 0} \phi_{\mathbf{U}} \mathrm{d}\mathbf{u} \end{aligned} \tag{4}$$

and may be integrated using the MCS method on random samples. Nevertheless, for example, a 10% confidence level of a targeted probability around 10^{-9} requires $\approx 10^{11}$ performance function evaluations limiting the application of MCS for damage tolerance analysis.

Figure 5b illustrates the performance function evolution in the standard space for the damage tolerance reliability analysis of a cracked beam in traction considering two random variables (Figure 5a). In the failure region, the gradient is close to zero impacting negatively the performance of the gradient-based optimization algorithm required for FORM. Moreover, the non-positive M_{FAD} values form a plateau where only the sign of $H(\mathbf{U})$ is available. The

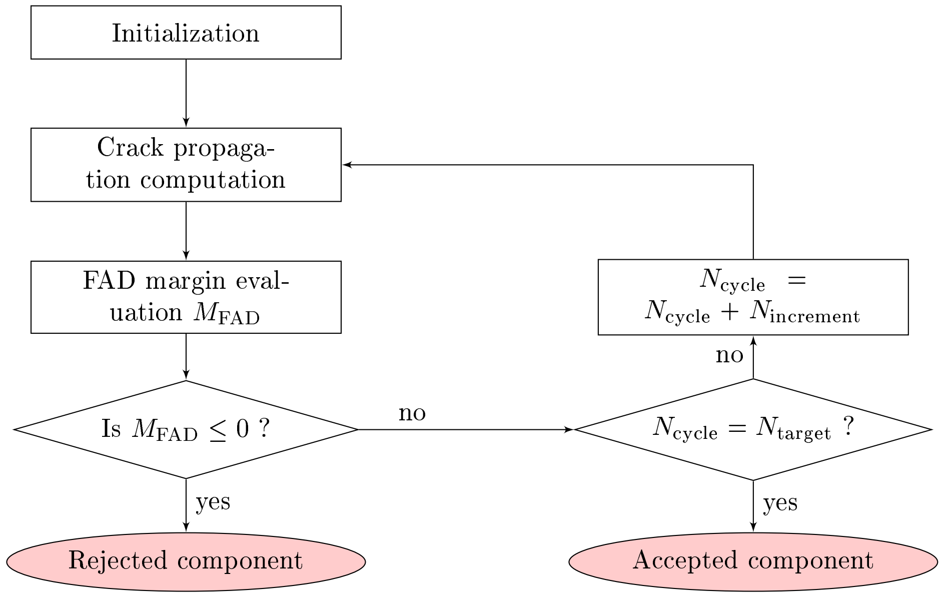

Figure 4: Algorithm of the damage tolerance procedure considered for this paper.

regression-based methods have difficulties establishing $H(\mathbf{U}) = 0$. Thus, this is the motivation for the development of a hybrid method detailed in the following section.

3. Methodology to evaluate the probability of failure

This section presents an adaptive strategy combining regression and classification approaches to assess the probability of failure within the damage tolerance hypothesis. The algorithm, based on the Subset Simulation principle [13], is divided into two phases:

- in the exploration phase, a regression-based approach is coupled with active learning [29]; the trends of the model are accounted to characterize intermediate thresholds;
- in the exploitation phase, a classification-based approach is associated with adaptive strategy because of the lack of quantitative information in the failure space; the goal is to accurately determine the limit state in the last iteration.

This hybrid 'Adaptive Regression and Classification' algorithm is based on Subset Simulation (ARC-Subset). The following paragraphs firstly describe the regression steps. Then, the classification is detailed and an active learning for classification based on the multi-objective optimization is proposed. The

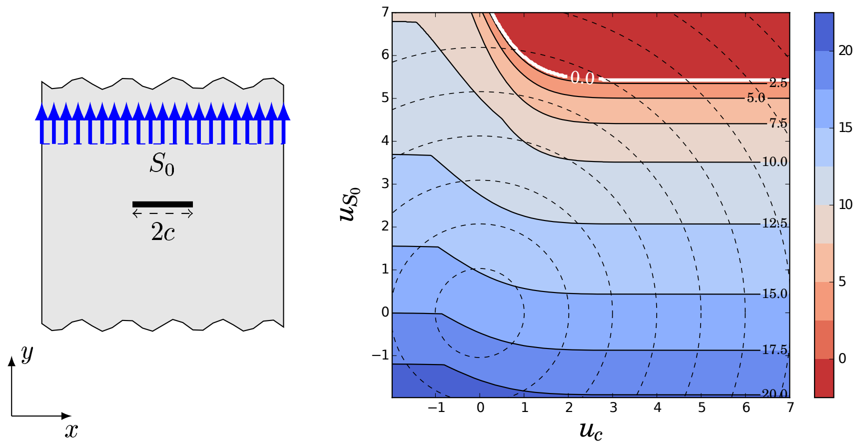

(a) (b)

Figure 5: 5a: Cracked beam in traction.
5b: Performance function in the $\mathbb{U}$ space for a through crack in a beam in traction using NASGRO [2]. Two random variables are considered: the length of the crack $c \sim \mathcal{U}[0.1\text{mm}; 1\text{mm}]$ and the load $S_0 \sim \mathcal{N}(52.5\text{MPa}; 10\%)$. Note the dashed circle lines representing the iso-values of standard deviation to give information about the distance to the failure region.

crucial point is the transition phase between the regression and classification steps (Section 3.3).

3.1. Regression phase

Figure 6 and Algorithm 1 respectively provide the flowchart and the pseudo-code of the regression part of the ARC-Subset. The initial DOE (b) is generated using optimized sampling or expert judgement and evaluated (c) to identify the global trends of the model based on the first subset population (a). A Kriging regression surrogate $\tilde{H}_{\text{Krig}}(\mathbf{u})$ is trained on the DOE (d) and is used to evaluate the subset population $\mathbf{u}_{\text{SS}}^{(k_{\text{SS}})}$ (e). The intermediate thresholds $q_{\text{th}}^{(k_{\text{SS}})}$ (f) are determined such as:

$$p_{k_{\text{SS}}} = P\left(\tilde{H}_{\text{Krig}}(\mathbf{U}) \leq q_{\text{th}}^{(k_{\text{SS}})}\right) = 0.1, \tag{5}$$

where $p_{k_{\text{SS}}}$ are intermediate subset probabilities. To improve the quality of the surrogate, enrichment strategies are employed (g') until quality stopping criteria are satisfied (g). If the transition criteria are not satisfied (h), a new subset population is generated (h'). The DOE is enriched selecting $2 \times d$ experiments by *k-means* clustering [40] of the new subset population (h").

The DOE is enriched by Adaptive Kriging (AK) [29] chosen for its simplicity and efficiency. Nevertheless, the AK stopping criterion proposed in [29] seems

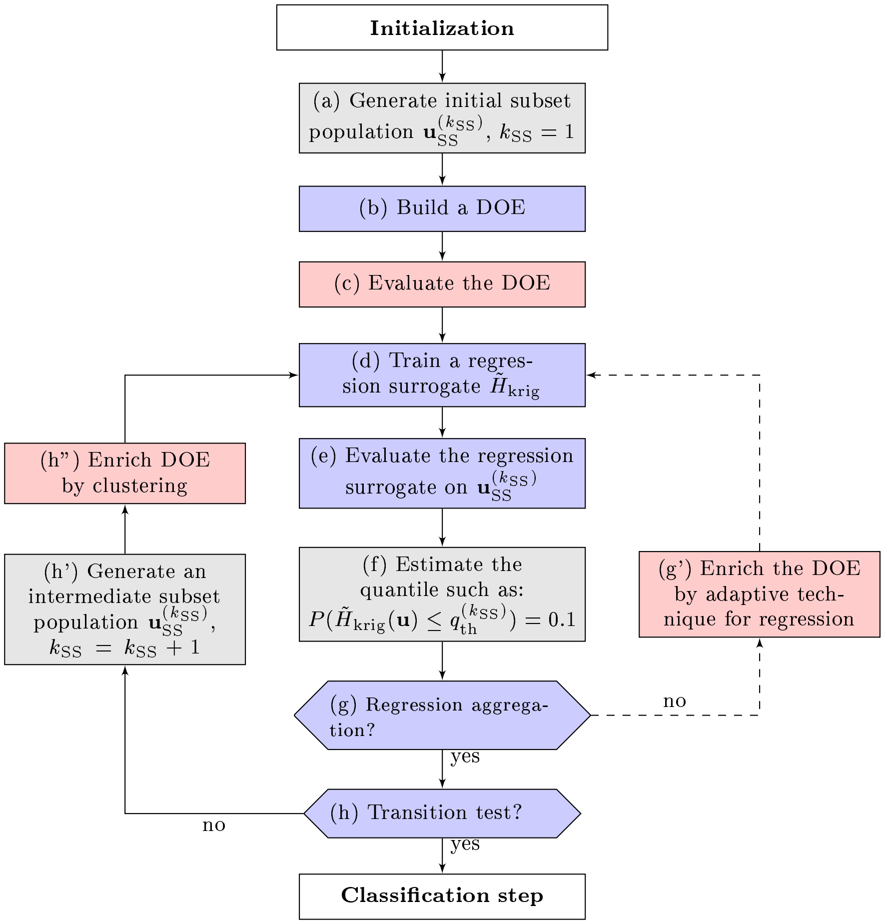

Figure 6: Regression steps of the ARC-Subset algorithm. The grey, blue and red boxes illustrate respectively Subset Simulation, surrogate and model requirements.

to be too conservative for first subset steps. As the goal is to cross these steps quickly, Tong [31] presents a new stopping criterion for threshold convergence adapted for the Subset Simulation context.

3.2. Classification phase

Due to LEFM hypothesis, the model does not provide quantitative information for failed experiments. An alternative way to identify the limit state is to use SVM classification, based solely on the sign of the performance function. At this step:

- the DOE contains at least one failed experiment,
- the subset population is the last population generated by the regression step.

3.2.1. Description of the algorithms

The flowchart of the classification part of the ARC-Subset methodology is detailed in Figure 7 and the pseudo-code is given in Algorithm 2. The DOE is

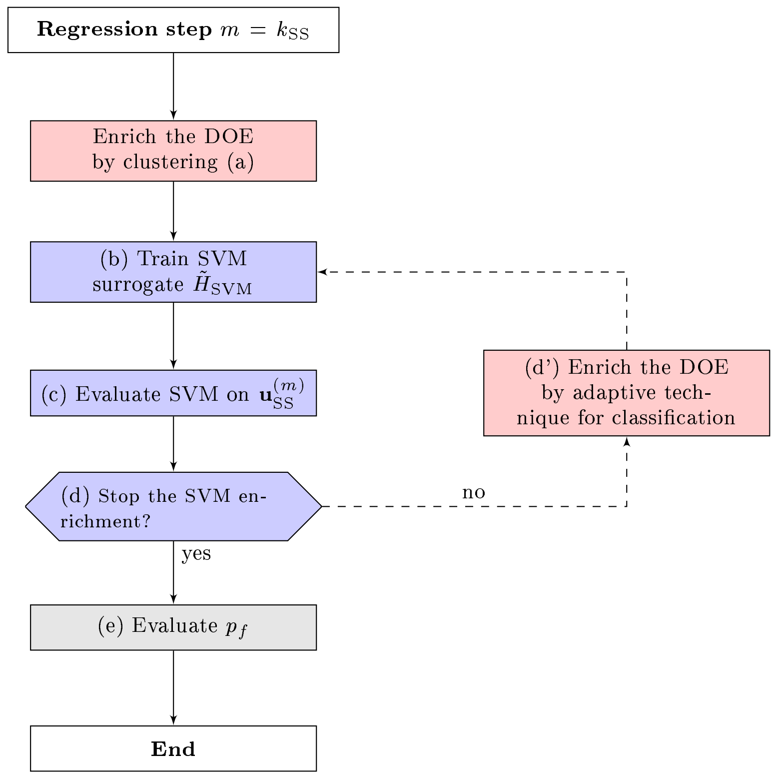

Figure 7: Classification step of the ARC-Subset algorithm. Color meaning is given in Figure 6.

enriched by *k-means* clustering of the last subset population (a) in order to train a SVM separator (b) to assess the final subset probability p_m (e) by surrogate evaluation (c)

$$p_m = \sum_{j=1}^{n_{\mathrm{SS}}} \mathbb{I}_{\tilde{H}_{\mathrm{SVM}}(\mathbf{u}_{\mathrm{SS}}^{(m)}) \leq 0} \tag{6}$$

in order to assess the probability of failure:

$$p_f = \prod_{k_{\mathrm{SS}}=1}^{m} p_{k_{\mathrm{SS}}}. \tag{7}$$

If the quality criterion of the SVM separator (d) is not achieved, the DOE is enriched (d') by the adaptive method improved for classification, presented in the next paragraph. Otherwise, the ARC-Subset stops and the reliability information is returned.

As the last classification step determines the quality of the reliability assessment, this paper proposes an enrichment strategy based on a compromise between exploration and exploitation.

3.2.2. Enrichment strategy

At this stage, the DOE contains experiments of both classes. The SVM separator defines the limit state, but it may suffer from a lack of accuracy around the zone of interest. Enrichment strategies for SVM are developed, principally based on the distance from the DOE. A multi-objective approach proposed in this section couples two criteria: a distance-based criterion and the probability of misclassification.

Distance-based criterion. To improve the accuracy of a boundary, Basudhar [35] proposes the Max-Min criterion based on the distance from the DOE coupled with a constraint on the distance from the SVM separator. The new experiment is selected by solving the following constrained optimization problem

$$\begin{aligned} \mathbf{u}_{\mathrm{MM}} \quad &= \arg\max_{\mathbf{u}} \min_{i=1\ldots n_{\mathrm{DOE}}} \|\mathbf{u}-\mathbf{u}_{\mathrm{DOE}}\| \\ \text{s.t.} \quad &\tilde{H}_{\mathrm{SVM}}(\mathbf{u}) = 0. \end{aligned} \tag{8}$$

This exploration approach is efficient enough to globally describe the limit state, but it does not account for the proximity to the center of the standard space. The generalized Max-Min is introduced by Lacaze [36] by multiplying the objective (8) by the joint density function $\phi_{\mathbf{U}}$

$$\begin{aligned} \mathbf{u}_{\mathrm{GMM}} \quad &= \arg\max_{\mathbf{u}} \min_{i=1\ldots n_{\mathrm{DOE}}} \|\mathbf{u}-\mathbf{u}_{\mathrm{DOE}}\| \times \phi_{\mathbf{U}}^{\frac{1}{d}} \\ \text{s.t.} \quad &\tilde{H}_{\mathrm{SVM}}(\mathbf{u}) = 0. \end{aligned} \tag{9}$$

Both optimizations may be solved by a local optimizer using the Chebychev norm.

Probability of misclassification. The SVM classifier aims at building a binary decomposition of the standard space. Platt [41] introduces the notion of the Probabilistic SVM (PSVM) which gives the probability of a point to belong to a given class. It proposes the sigmoid formulation mainly based on the distance to the separator

$$P(+1|\mathbf{u}) = \frac{1}{1+\exp(A\tilde{H}_{\mathrm{SVM}}(\mathbf{u})+B)}, \tag{10}$$

where A and B are deterministic PSVM parameters obtained by maximum likelihood. Basudhar [39] improves this model introducing the Distance PSVM (DPSVM)

$$P(+1|\mathbf{u}) = \frac{1}{1+\exp(A\tilde{H}_{\mathrm{SVM}}(\mathbf{u})+B(\frac{d_-}{d_+ + \tau_{\mathrm{PSVM}}} - \frac{d_+}{d_- + \tau_{\mathrm{PSVM}}}))}, \tag{11}$$

where τ_{PSVM} is a conditioning parameter, and d_+ and d_- are respectively the distance to the closest positive and negative experiments.

Consequently, it is possible to define the probability of misclassification $P_{\mathrm{mc}}(\mathbf{u})$. Basudhar [39] includes this notion to select a new experiment which has a high probability of being misclassified.

This paper proposes to combine both Max-Min criteria interpreted either as an exploration for the classical Max-Min or exploitation for the generalized one. The idea is to solve both optimization problems simultaneously and then select the new experiment which has the highest probability of misclassification. The next evaluated experiment is

$$\mathbf{u}_{\mathrm{new}} = \arg\max\left(P_{\mathrm{mc}}(\mathbf{u})\right), \quad \mathbf{u} \in \{\mathbf{u}_{\mathrm{MM}}, \mathbf{u}_{\mathrm{GMM}}\}. \tag{12}$$

In this approach, a compromise between exploration and exploitation is based on the probability of misclassification.

3.3. Transition between the regression and classification phases

One of the main points of ARC-Subset is to determine when the transition between regression and classification happens. When the limit state is achieved, the Subset Simulation criterion

$$q_{\mathrm{th}}^{(m)} \leq 0 \tag{13}$$

may be corrupted by the regression model if it is trained on a DOE containing failure experiments. A second criterion prevents a worse evaluation of the threshold due to failed experiments. The classification phase starts when k failure experiments are evaluated

$$\sum_{k=1}^{n_{\mathrm{DOE}}} \mathbb{I}_{H(\mathbf{u}_{\mathrm{DOE}}^{(k)})\leq 0} < k_{\mathrm{DOE}} \tag{14}$$

where $\mathbb{I}_{H(\mathbf{U})\leq 0}$ is the indicator function. In the following, k_{DOE} is arbitrarily set to twice, the dimension of the reliability problem. The pseudo-code of the transition phase is given in Algorithm 3.

4. Application to damage tolerance analysis

ARC-Subset methodology is applied applied to test cases based on NASGRO [2], a damage tolerance tool allowing to assess the FAD margin of a component after crack propagation when the targeted lifetime is reached or when the FAL is crossed (Section 2.1). The goal is to limit the number of damage tolerance evaluations required to assess low probabilities comparing with reference methods such as Subset Simulation [13] and *2SMART* [37]. The failure scenarios (1) and (2) are correlated using the R6 rule and the FAL is defined within same limits for the following test cases. The first case concerns a through crack and the second one refers to a surface crack in a beam.

Table 1: Properties of input random variables for the Through Crack in a beam

Variable	Distribution Type	Mean	Standard deviation
c	Uniform	0.55 mm	0.26 mm
S_0	Normal	52.5 MPa	5.25 MPa

4.1. Through Crack in a beam

The first case considers a through-crack in a beam in traction (type TC11 in NASGRO, Figure 5a). Two of the most significant variables are set as random: the size of the defect c and the load magnitude S_0. Table 1 describes the distribution of parameters. The ARC-Subset is compared with the classical Subset Simulation [13], adapted for low probability estimation. *2SMART* [37] is also applied to complete the comparison. This method combines SVM and Subset Simulation to reduce the number of model evaluations for low probabilities.

Table 2: Results of the through crack in a tension beam considering two random variables.

Method	Evaluations	p_f
Subset Simulation (10000/step)	104889	1.53×10^{-9} (8.64%)
2SMART [37]	3089	1.54×10^{-9}
ARC-Subset ($\times$10)	103.8 (8%)	1.55×10^{-9} (8.58%)

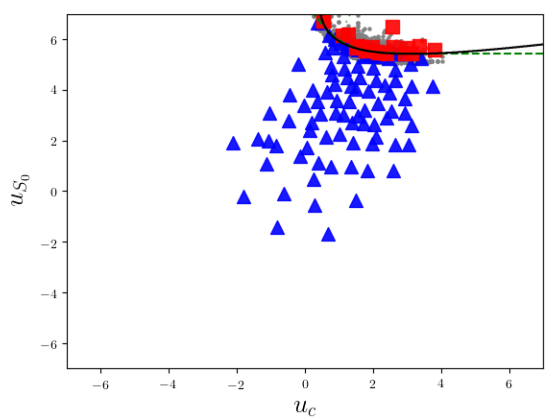

Figure 8: Damage tolerance evaluations required by ARC-Subset in the standard space. The blue triangle markers are the safe evaluations, and the red circles are failed ones. The green dashed line represents the actual limit state, and the solid black line is the one obtained by SVM.

Figure 8 shows in the standard space the 115 damage tolerance evaluation sites required by ARC-Subset to compute the failure probability 1.55×10^{-9}

with 8.58% confidence level. An example of the convergence of the last intermediate probability based on the SVM separator is given in Figure 9. Results are presented in Table 2. To get a similar probability of failure, the classical Subset Simulation and *2SMART* need respectively 104889 and 3089 damage tolerance evaluations. The number of model calls is thus reduced by respectively about 1000 and 20. The performances of ARC-Subset and *2SMART* are explained by the fact that, unlike Subset Simulation, damage tolerance model is replaced by a surrogate. The model evaluations are only required to build the

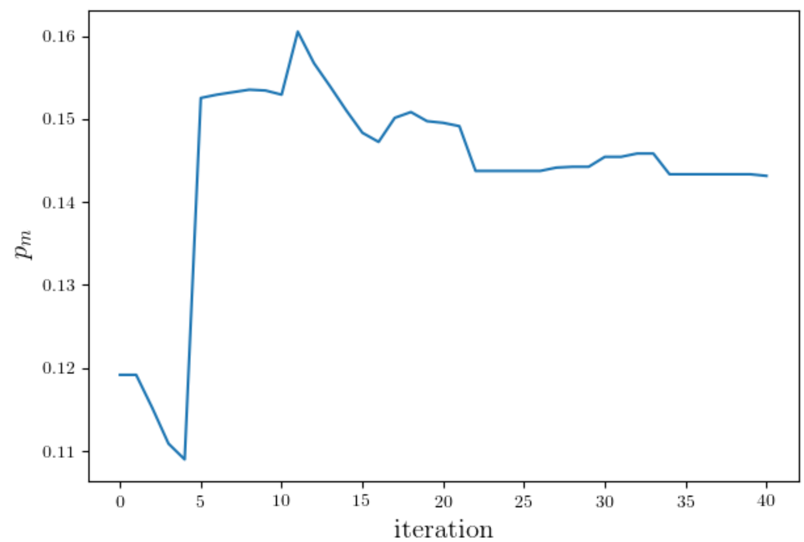

Figure 9: Evolution of the last subset intermediate probability p_m, computed using the SVM separator, for the last 40 iterations of ARC-Subset for the Through Crack test case until to convergence.

intermediate separators. Therefore, when the margin is positive, we can assume that regression surrogates are more efficient than classification. This explains why the ARC-Subset is more efficient than *2SMART* which needs an important number of experiments to describe intermediate subset limit states.

4.2. Surface Crack in a beam with 9 random variables

A surface crack in a beam is shown in Figure 10 (type SC17 in NASGRO). Nine parameters are set as random variables. The three methods provide nearly the same probability of failure at 1.19×10^{-7}(Table 3). As for the first test case, the ARC-Subset method saves respectively one and three orders of magnitude regarding the number of simulations compared to *2SMART* and Subset Simulation. Even if the target probability is higher than in the first example, the ARC-Subset requires more damage tolerance evaluations, due to the higher

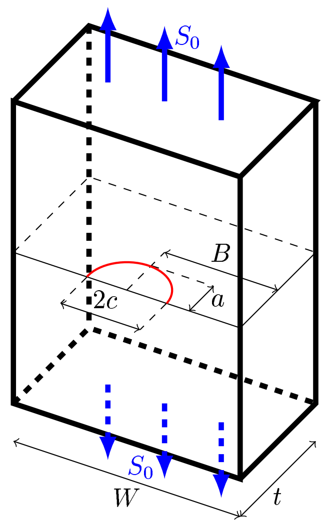

Figure 10: Surface Crack beam in traction [2].

Table 3: Results of the surface crack beam in traction considering nine random variables.

Method	Evaluations	p_f
Subset Simulation (10000/step)	81978	1.19×10^{-7} (11%)
2SMART [37]	4808	1.21×10^{-7}
ARC-Subset($\times$10)	479.6	1.40×10^{-7} (11%)

dimension of the problem, making the trends of the model more difficult to estimate in the regression phase. Despite this point, ARC-Subset is still able to assess the probability of failure while reducing the number of damage tolerance model evaluations.

The advantage of ARC-Subset is the possibility to assess a low probability of failure with a reduced number of simulations without quantitative information from failed experiments. This method can be extended to prevent code crash considering it as failed experiment defined as a qualitative information. The main limitation of this methodology is the curse of dimensionality which mainly impacts the regression phase. However, the modularity allows using a more suitable regression surrogate. Moreover, the confidence about p_f is based on the Subset Simulation estimators computed on the surrogates. The SVM separator gives no confidence level because the SVM margin, interpreted as a zone of uncertainty, is only based on support vectors and not on the whole DOE as it is the case for the Kriging variance. Therefore, this information is not available to estimate the confidence bounds of p_f.

5. Conclusion

The ARC-Subset methodology provides promising performance for damage tolerance applications by reducing the number of model evaluations while keeping the same level of accuracy as existing approaches. Nevertheless, we can identify some limitations. The test cases, even if issued from industrial practice, are of a relatively low complexity from the computational point of view. The scalability of the proposed approach is limited to relatively low dimensional applications due to the use of Kriging. Future work concerns the application of ARC-Subset on more complex test cases based on the extended finite element method (XFEM). The enrichment strategy may be further improved using a multi-objective optimization of both Max-Min criteria. Moreover, the extension of the ARC-Subset requires surrogate models better adapted to large dimensions.

Acknowledgments

The authors acknowledge the support of CNES (French National Center for Space Studies) and of ANRT (French National Association for Research and Technology) by the CIFRE convention 2015/0209. This work has been also partially supported by the ORFI project co-funded by the Walloon Region (Convention 7567).

References

[1] I. Milne, R. Ainsworth, A. Dowling, A. Stewart, Assessment of the integrity of structures containing defects, International Journal of Pressure Vessels and Piping 32 (1) (1988) 3–104.

[2] NASGRO, Fracture mechanics and fatigue crack growth analysis software version 7.1 - reference manual (2014).

[3] S. Bordas, B. Moran, Enriched finite elements and level sets for damage tolerance assessment of complex structures, Engineering Fracture Mechanics 73 (9) (2006) 1176–1201.

[4] S. Bordas, T. Rabczuk, G. Zi, Three-dimensional crack initiation, propagation, branching and junction in non-linear materials by an extended meshfree method without asymptotic enrichment, Engineering Fracture Mechanics 75 (5) (2008) 943–960.

[5] E. Wyart, M. Duflot, D. Coulon, P. Martiny, T. Pardoen, J.-F. Remacle, F. Lani, Substructuring fe–xfe approaches applied to three-dimensional crack propagation, Journal of Computational and Applied Mathematics 215 (2) (2008) 626–638.

[6] D. Virkler, B. Hillberry, P. Goel, The statistical nature of fatigue crack propagation, Journal of Engineering Materials and Technology 101 (2) (1979) 148–153.

[7] C. Mattrand, J.-M. Bourinet, Random load sequences and stochastic crack growth based on measured load data, Engineering Fracture Mechanics 78 (17) (2011) 3030–3048.

[8] F. Grooteman, A stochastic approach to determine lifetimes and inspection schemes for aircraft components, International Journal of Fatigue 30 (1) (2008) 138–149.

[9] W. Greenwood, K. Chase, A new tolerance analysis method for designers and manufacturers, Journal of Engineering for Industry 109 (2) (1987) 112–116.

[10] S. Sankararaman, Y. Ling, S. Mahadevan, Uncertainty quantification and model validation of fatigue crack growth prediction, Engineering Fracture Mechanics 78 (7) (2011) 1487–1504.

[11] B. Echard, N. Gayton, M. Lemaire, M. Afzali, A. Bignonnet, P. Boucard, G. Defaux, J. Dulong, A. Ghouali, F. Lefebvre, Reliability assessment of an aerospace component subjected to fatigue loadings: Approfi project, 4th Fatigue Design.

[12] A. Altamura, D. Straub, Reliability assessment of high cycle fatigue under variable amplitude loading: Review and solutions, Engineering Fracture Mechanics 121 (2014) 40–66.

[13] S.-K. Au, J. Beck, Estimation of small failure probabilities in high dimensions by subset simulation, Probabilistic Engineering Mechanics 16 (4) (2001) 263–277.

[14] K. A. Cliffe, M. B. Giles, R. Scheichl, A. L. Teckentrup, Multilevel monte carlo methods and applications to elliptic pdes with random coefficients, Computing and Visualization in Science 14 (1) (2011) 3.

[15] P. Hauseux, J. S. Hale, S. P. Bordas, Accelerating monte carlo estimation with derivatives of high-level finite element models, Computer Methods in Applied Mechanics and Engineering 318 (2017) 917–936.

[16] L. L. Gratiet, J. Garnier, Recursive co-kriging model for design of cumputer experiments multiple levels of fidelity, International Journal for Uncertainty Quantification 4 (5) (2014) 365–386.

[17] T. Benamara, P. Breitkopf, I. Lepot, C. Sainvitu, Adaptive infill sampling criterion for multi-fidelity optimization based on gappy-pod, Structural and Multidisciplinary Optimization 54 (4) (2016) 843–855.

[18] Y. Zhang, A. Der Kiureghian, Two improved algorithms for reliability analysis (1995) 297–304.

[19] A. Der Kiureghian, T. Dakessian, Multiple design points in first and second-order reliability, Structural Safety 20 (1) (1998) 37–49.

[20] B. Fiessler, R. Rackwitz, H.-J. Neumann, Quadratic limit states in structural reliability, Journal of the Engineering Mechanics Division 105 (4) (1979) 661–676.

[21] J. C. Helton, F. J. Davis, Latin hypercube sampling and the propagation of uncertainty in analyses of complex systems, Reliability Engineering & System Safety 81 (1) (2003) 23–69.

[22] V. J. Romero, J. V. Burkardt, M. D. Gunzburger, J. S. Peterson, Comparison of pure and latinized centroidal voronoi tessellation against various other statistical sampling methods, Reliability Engineering & System Safety 91 (10) (2006) 1266–1280.

[23] P. Das, Y. Zheng, Cumulative formation of response surface and its use in reliability analysis, Probabilistic Engineering Mechanics 15 (4) (2000) 309–315.

[24] N. Gayton, J. Bourinet, M. Lemaire, Cq2rs: a new statistical approach to the response surface method for reliability analysis, Structural safety 25 (1) (2003) 99–121.

[25] P. Zhang, P. Breitkopf, C. Knopf-Lenoir, W. Zhang, Diffuse response surface model based on moving latin hypercube patterns for reliability-based design optimization of ultrahigh strength steel nc milling parameters, Structural and Multidisciplinary Optimization 44 (5) (2011) 613–628.

[26] I. Kaymaz, Application of kriging method to structural reliability problems, Structural Safety 27 (2) (2005) 133–151.

[27] M. Balesdent, J. Morio, J. Marzat, Kriging-based adaptive importance sampling algorithms for rare event estimation, Structural Safety 44 (2013) 1–10.

[28] B. Bichon, M. Eldred, L. Swiler, S. Mahadevan, J. McFarland, Efficient global reliability analysis for nonlinear implicit performance functions, AIAA journal 46 (10) (2008) 2459–2468.

[29] B. Echard, N. Gayton, M. Lemaire, Ak-mcs: an active learning reliability method combining kriging and monte carlo simulation, Structural Safety 33 (2) (2011) 145–154.

[30] X. Huang, J. Chen, H. Zhu, Assessing small failure probabilities by ak–ss: an active learning method combining kriging and subset simulation, Structural Safety 59 (2016) 86–95.

[31] C. Tong, Z. Sun, Q. Zhao, Q. Wang, S. Wang, A hybrid algorithm for reliability analysis combining kriging and subset simulation importance sampling, Journal of Mechanical Science and Technology 29 (8) (2015) 3183–3193.

[32] J. Hurtado, Structural reliability: statistical learning perspectives, Vol. 17, Springer Science & Business Media, 2013.

[33] H. Song, K. Choi, I. Lee, L. Zhao, D. Lamb, Adaptive virtual support vector machine for reliability analysis of high-dimensional problems, Structural and Multidisciplinary Optimization 47 (4) (2013) 479–491.

[34] Q. Pan, D. Dias, An efficient reliability method combining adaptive support vector machine and monte carlo simulation, Structural Safety 67 (2017) 85–95.

[35] A. Basudhar, S. Missoum, An improved adaptive sampling scheme for the construction of explicit boundaries, Structural and Multidisciplinary Optimization 42 (4) (2010) 517–529.

[36] S. Lacaze, S. Missoum, A generalized max-min sample for surrogate update, Structural and Multidisciplinary Optimization 49 (4) (2014) 683–687.

[37] J. Bourinet, F. Deheeger, M. Lemaire, Assessing small failure probabilities by combined subset simulation and support vector machines, Structural Safety 33 (6) (2011) 343–353.

[38] J. Bourinet, Rare-event probability estimation with adaptive support vector regression surrogates, Reliability Engineering & System Safety 150 (2016) 210–221.

[39] A. Basudhar, C. Dribusch, S. Lacaze, S. Missoum, Constrained efficient global optimization with support vector machines, Structural and Multidisciplinary Optimization 46 (2) (2012) 201–221.

[40] J. MacQueen, et al., Some methods for classification and analysis of multivariate observations, in: Proceedings of the fifth Berkeley symposium on mathematical statistics and probability, Vol. 1, Oakland, CA, USA, 1967, pp. 281–297.

[41] J. Platt, Probabilistic outputs for support vector machines and comparisons to regularized likelihood methods, Advances in large margin classifiers 10 (3) (1999) 61–74.

[42] A. Basudhar, S. Missoum, Adaptive explicit decision functions for probabilistic design and optimization using support vector machines, Computers & Structures 86 (19) (2008) 1904–1917.

Algorithm 1 ARC-Subset pseudo-code algorithm of the regression phase

initialization $p_f = 1$, $k_{\mathrm{SS}} = 1$, $p_{\mathrm{target}} = 0.1$, $n_{\mathrm{DOE}} = 5 \times d$, $n_{\mathrm{SS}} = 10e4$
    ▷ Preconised settings (User can modify it according to expert judgement)
test$_{\mathrm{transition}} \leftarrow$ `False`
while test$_{\mathrm{transition}} =$ `False` **do**
    if $k_{\mathrm{SS}} = 1$ **then**
        Generate $\mathbf{u}_{\mathrm{SS}}^{(k_{\mathrm{SS}})} \sim \phi_{\mathbf{U}}$
        $\mathbf{u}_{\mathrm{DOE}} \leftarrow n_{\mathrm{DOE}}$-clusters of $\mathbf{u}_{\mathrm{SS}}^{(k_{\mathrm{SS}})}$
        Evaluate $H(\mathbf{u}_{\mathrm{DOE}})$
    else
        Generate $\mathbf{u}_{\mathrm{SS}}^{(k_{\mathrm{SS}})}$ using *modified* Metropolis Hastings algorithm [13]
        $\mathbf{u}_{\mathrm{new}} \leftarrow k_{\mathrm{new}}$-clusters of $\mathbf{u}_{\mathrm{SS}}^{(k_{\mathrm{SS}})} | \tilde{H}_{k_{\mathrm{SS}}}(\mathbf{u}_{\mathrm{SS}}^{(k_{\mathrm{SS}})}) < q_{\mathrm{th}}^{(k_{\mathrm{SS}})}$
        Evaluate $H(\mathbf{u}_{\mathrm{new}})$ and $\mathbf{u}_{\mathrm{DOE}} \leftarrow \mathbf{u}_{\mathrm{DOE}} \cup \mathbf{u}_{\mathrm{new}}$
        test$_{\mathrm{Krig}} \leftarrow$ CheckTransition $\left(\mathbf{u}_{\mathrm{DOE}}, q_{\mathrm{th}}^{(k_{\mathrm{SS}})}\right)$
    end if
    test$_{\mathrm{Krig}} \leftarrow$ `False`
    while test$_{\mathrm{Krig}} =$ `False` **do**
        Train a Kriging surrogate $\tilde{H}_{\mathrm{Krig}}$ on $\mathbf{u}_{\mathrm{DOE}}$
        Evaluate $\tilde{H}_{\mathrm{Krig}}(\mathbf{u}_{\mathrm{SS}}^{(k_{\mathrm{SS}})})$
        Estimate $q_{\mathrm{th}}^{(k_{\mathrm{SS}})}$ such as $P(H((\mathbf{u}_{\mathrm{SS}}^{(k_{\mathrm{SS}})})) \leq q_{\mathrm{th}}^{(k_{\mathrm{SS}})}) = p_{\mathrm{target}}$
        Compute $\eta_{\mathrm{AK}}(\mathbf{u}_{\mathrm{SS}}^{(k_{\mathrm{SS}})}) = \frac{\left|q_{\mathrm{th}}^{(k_{\mathrm{SS}})} - \tilde{H}_{\mathrm{Krig}}(\mathbf{u}_{\mathrm{SS}}^{(k_{\mathrm{SS}})})\right|}{\sigma_{\mathrm{Krig}}(\mathbf{u}_{\mathrm{SS}}^{(k_{\mathrm{SS}})})}$
        Check test$_{\mathrm{Krig}}$ [31]
        if test$_{\mathrm{Krig}} =$ `False` **then**
            $\mathbf{u}_{\mathrm{AK}} \leftarrow \min \eta_{\mathrm{AK}}(\mathbf{u}_{\mathrm{SS}}^{(k_{\mathrm{SS}})})$
            Evaluate $H(\mathbf{u}_{\mathrm{AK}})$ and $\mathbf{u}_{\mathrm{DOE}} \leftarrow \mathbf{u}_{\mathrm{DOE}} \cup \mathbf{u}_{\mathrm{AK}}$
        end if
        test$_{\mathrm{Krig}} \leftarrow$ CheckTransition $\left(\mathbf{u}_{\mathrm{DOE}}, q_{\mathrm{th}}^{(k_{\mathrm{SS}})}\right)$
    end while
    $p_f \leftarrow p_f \times p_{\mathrm{target}}$ and $k_{\mathrm{SS}} \leftarrow k_{\mathrm{SS}} + 1$
end while

Algorithm 2 ARC-Subset pseudo-code algorithm of the classification phase

at this step p_f, $m \leftarrow k_{\mathrm{SS}}$, $\mathbf{u}_{\mathrm{SS}}^{(m)}$
$\mathrm{test}_{\mathrm{SVM}} \leftarrow$ `False`
while $\mathrm{test}_{\mathrm{SVM}} =$ `False` **do**
  Train a SVM separator $\tilde{H}_{\mathrm{SVM}}$ on $\mathbf{u}_{\mathrm{DOE}}$
  Find $\mathbf{u}_{\mathrm{MM}}$ [35] and $\mathbf{u}_{\mathrm{GMM}}$ [36] (Optimization)
  $\mathbf{u}_{\mathrm{new}} \leftarrow \arg\max\left(P_{\mathrm{mc}}(\mathbf{u})\right), \quad \mathbf{u} \in \{\mathbf{u}_{\mathrm{MM}}, \mathbf{u}_{\mathrm{GMM}}\}$ (Section 3.2.2)
  Evaluate $H(\mathbf{u}_{\mathrm{new}})$ and $\mathbf{u}_{\mathrm{DOE}} \leftarrow \mathbf{u}_{\mathrm{new}} \cup \mathbf{u}_{\mathrm{AK}}$
  Check $\mathrm{test}_{\mathrm{SVM}}$ [42]
end while
$p_m = P\left(\tilde{H}_{\mathrm{SVM}} \leq 0\right)$
end $p_f = p_f \times p_m$

Algorithm 3 Pseudo-code of the transition test

function CheckTransition($\mathbf{u}_{\mathrm{DOE}}$, $q_{\mathrm{th}}^{(k_{\mathrm{SS}})}$)
  if $\sum_{k=1}^{n_{\mathrm{DOE}}} \mathbb{I}_{H(\mathbf{u}_{\mathrm{DOE}})\leq 0} \geq k_{\mathrm{DOE}}$ or $q_{\mathrm{th}}^{(k_{\mathrm{SS}})} \leq 0$ **then**
  ▷ By default $k_{\mathrm{DOE}} = 2 \times d$
    $\mathrm{test}_{\mathrm{transition}} =$ `True`
    go to classification phase
  else
    $\mathrm{test}_{\mathrm{transition}} =$ `False`
  end if
  return $\mathrm{test}_{\mathrm{transition}}$
end function